Biogeochemistry (2009) 93:31–48
DOI 10.1007/s10533-008-9271-y

Modeling N_2O flux from an Illinois agroecosystem using Monte Carlo sampling of field observations

Christina Tonitto · Mark B. David · Laurie E. Drinkwater

Received: 11 February 2008 / Accepted: 9 June 2008 / Published online: 8 January 2009

Abstract We modeled the expected range of seasonal and annual N_2O flux from temperate, grain agroecosystems using Monte Carlo sampling of N_2O flux field observations. This analysis is complimentary to mechanistic biogeochemical model outcomes and provides an alternative method of estimating N_2O flux. Our analysis produced a range of annual N_2O gas flux estimates with mean values overlapping with results from an intermodel comparison of mechanistic models. Mean seasonal N_2O flux was 1–4% of available N, while median seasonal N_2O flux was less than 2% of available N across corn, soybean, wheat, ryegrass, legume, and bare fallow systems. The 25th–75th percentile values for simulated average annualized N_2O flux rates ranged from 1 to 12.2 kg N ha^{-1} in the conventional system, from 1.3 to 8.8 kg N ha^{-1} in the cover crop rotation, and from 0.8 to 9.3 kg N ha^{-1} in the legume rotation. Although these modeling techniques lack the seasonal resolution of mechanistic models, model outcomes are based on measured field observations. Given the large variation in seasonal N gas flux predictions resulting from the application of mechanistic simulation models, this data-derived approach is a complimentary benchmark for assessing the impact of agricultural policy on greenhouse gas emissions.

Keywords Nitrogen · Nitrous oxide · N trace gas · Corn Belt

C. Tonitto (✉)
Department of Ecology and Evolutionary Biology and Department of Horticulture, Cornell University, Ithaca, NY 14853, USA
e-mail: ctonitto@cornell.edu

M. B. David
Department of Natural Resources and Environmental Sciences, University of Illinois at Urbana-Champaign, W-503 Turner Hall, 1102 S. Goodwin Av., Urbana, IL 61801, USA

L. E. Drinkwater
Department of Horticulture, Cornell University, Ithaca, NY 14853, USA

Introduction

Nitrogen gas flux, in particular denitrification, is difficult to measure. The difficulty stems from both methodological limitations (Groffman et al. 2006), as well as the high spatial (Clemens et al. 1999) and temporal (e.g., McSwiney and Robertson 2005; Wagner-Riddle and Thurtell 1998) variability in field-scale N gas flux. In controlled environments, availability of C and N, and soil moisture or aerobic status are widely documented as important drivers of denitrification rates (del Prado et al. 2006; Firestone and Davidson 1989; Mathieu et al. 2006; Mosier et al. 1996; Wallenstein et al. 2006; Weier et al. 1993). Carbon availability and aerobic status are particularly

important in determining the partitioning of denitrification products into N_2O or N_2 (Weier et al. 1993). Agroecosystem management influences all of these soil environmental properties. Microbial community composition as a result of land management may further complicate N_2O flux dynamics. Cavigelli and Robertson (2000) demonstrated that agricultural land use history has a long-term effect on microbial community response to oxygen and pH with respect to enzymes involved in N_2O production.

Models are increasingly used to quantify landscape-scale N gas flux, especially to inform agricultural policy. In a broad review of ecosystem models which explicitly model denitrification, Heinen (2006) reports that there is no universally accepted approach to modeling N gas flux. Mechanistic terrestrial N cycle models derive their core mathematical description of flux between N redox states from biogeochemical process rates observed in controlled laboratory experiments conducted using soil cores (e.g., Li et al. 1992, 2007; Parton et al. 1987, 1998; Tague and Band 2004). However, there are few long-term data sets of N gas flux for use in model validation. Li et al. (2005) is one of few examples of rigorous comparison of N_2O flux observations against model outcomes. In this work the authors applied DAYCENT, DNDC, and WNMM N gas flux model frameworks and demonstrated all three models were able to simulate the timing of peak and low N_2O flux values. However, the models are not able to reliably capture the magnitude of peak events, resulting in r^2 values ranging from 0.14, 0.35, and 0.45 for DAYCENT, DNDC, and WNMM, respectively. The authors found it unexpected that the relatively simple WNMM model, which does not explicitly model soil gas diffusion, performed best based on the r^2 statistic. In general, however, model calibration is rarely constrained by known N gas flux or soil N storage measurements. Instead, model studies of N dynamics are generally bounded by known system N inputs via fertilization and deposition, and N export in crop yield and nitrate leaching (David et al. 2009). Model partitioning of excess N between N gas emissions and storage in soil pools remains a significant uncertainty in N cycle model outcomes. For the cases where we demonstrate that our simulations adequately reflect measured values of nitrate leaching and plant N, we need to better understand if we are getting the 'right' answer because our models accurately capture (1) the partitioning of excess N between storage in soil pools and N gas emissions, and (2) the spatial and temporal variation in N cycle processes and their resulting distribution across the landscape.

In the US, grain agroecosystems are managed as N-saturated systems with limited opportunity for nutrient recycling since animal and grain production is concentrated in different regions (Drinkwater and Snapp 2007). Productive land in the US Corn Belt receives substantial inorganic N additions (150–225 kg N ha^{-1} $year^{-1}$ for corn fields), resulting in a landscape where seasonal peaks in soil inorganic N status often coincide with peak precipitation events and high soil moisture status, creating conditions optimal for N gas loss, as well as nitrate leaching. Managing N_2O flux is a challenging question in this agroecosystem given our limited ability to predict the spatial and temporal distribution of environmental drivers (soil NO_3^- concentration, soil moisture status, C availability) as well as the true range of N gas flux under varying environmental conditions. From a policy perspective, due to the greenhouse gas properties of N_2O, we are interested in enhancing our ability to explicitly model the N_2O component of N gas flux, however many simulation model (Arnold et al. 1998; Gassman et al. 2005; Neitsch et al. 2005; Williams et al. 1983; Youssef 2003; Youssef et al. 2005) and mass balance model (David and Gentry 2000) approaches only predict net N gas loss. Can we identify land management scenarios with the highest contribution to N_2O flux? Can revised management scenarios reduce N_2O forcing and maintain viable yield?

In simulations of Illinois tile-drained corn-soybean agroecosystems, ephemeral events which result in optimal conditions for denitrification account for the majority of annual N gas loss (Tonitto et al. 2007b). These model results are supported by event-based N gas flux sampling which demonstrates extremely high flux when precipitation follows a fertilization event (Dobbie and Smith 2001; Li et al. 2002; Wagner-Riddle and Thurtell 1998). This event validation (Rykiel 1996) of N gas flux outcomes for Illinois agroecosystems bolstered confidence in DNDC model dynamics. While event validation quantifies model ability to simulate response to short-time-scale (daily) phenomena, confidence in long-time-scale (annual to decadal) model projections is desirable for

model application to land management. A recent comparison of widely applied biogeochemical models for this tile-drained Illinois corn-soybean agroecosystem demonstrated broad disagreement across the models tested in their simulation of N_2 and N_2O flux (David et al. 2009), raising questions about relying solely on simulation model outcomes to project agroecosystem N gas loss in space and time. Do mechanistic agroecosystem simulation models adequately integrate environmental drivers to describe aggregate N gas dynamics?

In this paper, we model potential annual N_2O gas flux across agricultural land management practices viable in Illinois agroecosystems by applying a Monte Carlo statistical sampling algorithm to field observations. Our goal was to provide an observation-based counterpoint to simulation model outcomes (David et al. 2009; Tonitto et al. 2007b) and N mass balance (David and Gentry 2000) approaches to quantifying N gas flux from agroecosystems.

Methods

Agroecosystem studied

We assessed the total N_2O flux from three grain cropping systems that are economically and ecologically viable in the US Corn Belt. The rotations contrasted were (number of months per land cover in parenthesis): (i) a two year rotation of corn (5.5), bare fallow (7), soybean (4.5), bare fallow (7), (ii) a two year rotation of corn (5.5), ryegrass cover crop (7), soybean (4.5), ryegrass cover crop (7), and (iii) a three year rotation of corn (5.5), ryegrass cover crop (7), soybean (4.5), winter wheat (9), and legume cover crop (10) (see Table 1 for a summary). The months attributed to each field management studied were derived from the schedule used in previous analyses of Illinois grain systems (David et al. 2009; Tonitto et al. 2007a, b). In order to simulate complete rotations across all land management scenarios studied, we modeled N_2O flux during a sample 6-year-period, equivalent to three implementations of the 2-year-rotations and two implementations of the 3-year-rotation. Because the legume database included fields with a mixture of legume and non-legume grasses, we considered the legume rotation to represent a best management practice in which maximum N-fixation was regulated by competition between an N-fixing and non-N-fixing grass.

Table 1 Management schedule for rotations simulated

Schedule	Rotation		
	Conventional	Cover crop	Legume
Year 1	Corn (5.5)	Corn (5.5)	Corn (5.5)
	Fallow (7)	Ryegrass (7)	Ryegrass (7)
Year 2	Soybean (4.5)	Soybean (4.5)	Soybean (4.5)
	Fallow (7)	Ryegrass (7)	Winter wheat (9)
Year 3			Legume (10)

Numbers in parentheses indicates months of a given land cover practice

Note: Each crop is listed in the year it is planted; in the case of ryegrass, winter wheat, and legume management the growing season extends into the subsequent calendar year. Similarly, fallow management straddles the fall, winter, and spring season between crop harvest and subsequent crop planting. The combined duration across management practices sums to either 24 or 36 months for a 2-year or 3-year-rotation, respectively

Data sources and summary statistics

We used the agricultural database compiled in Hofstra and Bouwman (2005) and Stehfest and Bouwman (2006) to model the probability distribution of annual N_2O flux from grain agroecosystems with rotations including fields managed for corn, soybean, ryegrass, wheat, legume and non-legume grasses, and bare fallow. While the complete data base contains all global ecosystems for which data are available, we only analyze data points for the crops and land management in the rotations described above. Extracted N_2O flux data met the following criteria: (1) from a temperate climate, (2) reported in units N mass area^{-1} time^{-1}, and (3) included explicit documentation of N fertilization rate. A total of 414 data points were used in this analysis; 75% of the data points were from long-term studies.

Figure 1 shows the distribution of climates represented in the data set. The USDA hardiness index is a standard metric for linking vegetation with a climate suitable for its growth. USDA hardiness zone 1 is the coldest climate, including the tundra, while lowland tropical ecosystems are in zone 13. Northern Illinois is in USDA hardiness zone 5 and southern Illinois is in hardiness zone 6. While the data span a range of climates, many observations are from climate zones 5

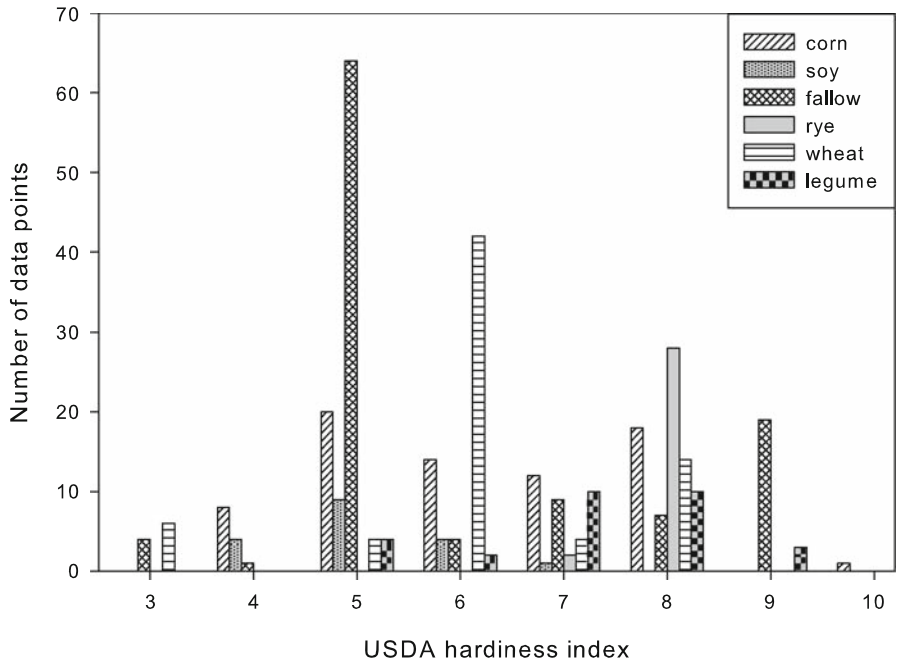

Fig. 1 Distribution of data points by climate. Data are presented by crop using the USDA hardiness index as an indicator of climate. Northern IL is in climate zone 5; southern IL is in climate zone 6

and 6. Observations in USDA hardiness zones 7 and 8 are predominantly from continental Europe, with growing season climate comparable to that of IL, but with a milder winter. Other data points in zone 7 and 8 are for the southeastern US. Data for ryegrass and legume crops are predominantly from climate zones 7 and 8. Because socioeconomic policies in Canada and the US support land management with significant bare fallow periods, there is limited data for winter cover crops in USDA hardiness zones 5 and 6.

The average duration of N_2O flux sampling was five months, which we consider representative of a growing or management season. Mean seasonal N_2O flux from the six land use categories studied ranged from 0.5 to 7.3 kg N ha^{-1} (Table 2). With the exception of wheat crops, all land cover types showed higher emissions in coarser, relative to finer, soil textures. Medium and coarse textured soils also showed a broad range of variation in terms of minimum and maximum seasonal N_2O emissions relative to fine textured soils.

Model framework

We developed a statistical model of the N_2O flux rate ($time^{-1}$) by applying a Monte Carlo sampling algorithm to these field observations to create probability distributions of N_2O emissions under different grain cropping systems. Though laboratory observations demonstrate that N_2O flux is sensitive to the soil environment, few publications document environmental drivers of N gas flux (e.g., C availability or aerobic status) under field conditions. As a result, we are unable to develop a mechanistic model based on field observations. Nonetheless, quantifying N_2O emissions using observation-based modeling provides insight which is distinctly different from outcomes based on mechanistic models derived from controlled laboratory experiments. Relative to controlled lab experiments, field observations integrate the effect of complex soil structure, complex plant rooting structure, plant-microbe interactions, dynamically varying moisture and temperature conditions, and uncertainty inherent in quantifying the spatial and temporal impact of land management practices, such as the extent to which the timing of land management coincides optimally or sub-optimally with climate events. Only field observations quantify the integrated effect of multiple, interacting factors on the range of N_2O flux observed under commercial farm operations. A model derived from field observations provides a comparison point for simulation-based model predictions. Given the limited availability of N_2O flux data in the US Corn Belt, additional N_2O flux comparison points are valuable for simulation model validation and development.

Table 2 Seasonal N_2O flux sorted by land cover type and soil texture (fine, medium, coarse). Median, mean, minimum, and maximum N_2O emissions (kg N ha^{-1}) for a five month (150 day) period based on values reported in the literature. (*ND* no data)

Texture	Seasonal N_2O emissions (kg N ha^{-1})					
	Corn	Soybean	Wheat	Ryegrass	Legume	Fallow
Fine						
Median	1.3	ND	2.3	ND	ND	0.7
Mean	1.6	ND	5.3	ND	ND	0.8
Minimum	0.7	ND	0.6	ND	ND	0.0
Maximum	2.8	ND	17.8	ND	ND	1.4
Observations	7	ND	6	ND	ND	6
Medium						
Median	0.7	1.4	0.4	0.5	0.3	1.3
Mean	3.0	1.5	0.5	0.7	0.6	4.7
Minimum	0.2	0.3	0.1	0.0	0.0	0.1
Maximum	16.0	3.2	1.1	2.6	1.8	78.9
Observations	15	6	15	29	9	50
Coarse						
Median	1.2	0.7	1.4	ND	0.8	1.9
Mean	3.1	3.7	2.2	ND	1.1	7.3
Minimum	−0.1	0.1	0.0	ND	0.1	0.0
Maximum	18.3	24.7	6.9	ND	6.3	92.8
Observations	44	8	29	ND	20	59

We applied a simple accounting model to estimate agroecosystem N_2O flux mass (kg N ha^{-1}) over the duration of a given rotation. We calculate N_2O flux for specific crop and soil texture categories. Model inputs derived from the database (Hofstra and Bouwman 2005; Stehfest and Bouwman 2006) were grouped according to the following soil texture categories: (1) fine for sandy clay, silty clay, or clay soils, (2) medium for sandy clay loam, clay loam, or silty clay loam soils, and (3) coarse for sand, loamy sand, sandy loam, loam, silt loam, or silt soils. From the database, we extracted field observations for corn, soybean, ryegrass, wheat, legume, and bare fallow land cover types.

Our modeling framework is organized as follows (details in subsequent paragraphs):

1. Extract N_2O flux field data from the database: (a) categorize by land cover, (b) subcategorize by soil texture.
2. Model N mineralization for each land cover category using the DNDC model.
3. Calculate the N_2O flux rate (Eq. 2) for each land cover and soil texture combination from the field N_2O flux data, field N fertilization inputs, and modeled N mineralization rates.
4. Calculate the N_2O flux mass (Eq. 1) for each land cover and soil texture combination by applying Monte Carlo simulation to compute statistical distributions for: (a) N_2O flux rate, (b) N mineralization rate, (c) N fertilization rate.
5. Calculate N_2O flux mass across each rotation by combining Eq. 1 outcomes from step 4 for each relevant land cover.

This framework depends on the following assumptions: (1) the lognormal and gamma distributions are a meaningful approximation of N_2O flux in the agricultural landscape, (2) the variation of N_2O flux documented in the published literature adequately bounds the range in flux possible in response to dynamic climate and soil environmental drivers, (3) modeled N mineralization is an adequate approximation of average N mineralization rate under the land management practices studied, (4) N_2O flux and N available distributions can be modeled as independent, (5) N fertilizer application rate and N mineralization distributions can be modeled as independent. The model calculations and justification of model assumptions are described in more detail in the subsequent section.

N_2O flux calculations

Equation 1 describes our simple accounting model for computing N_2O flux mass. We applied Eq. 1 using the N_2O flux rate defined in Eq. 2 and discussed in detail below. Our simple accounting model does not explicitly represent climate and soil environmental drivers. However, because the observations used to develop this model are from geographically diverse temperate grain agroecosystems and are categorized by soil texture, the simulation outcomes reflect potential N_2O flux mass covering a broad range of climatic and soil environmental conditions. Furthermore, Illinois climate and dominant soil texture is well represented in the field observations.

Furthermore, in many systems N mineralization accounts for about half of the N assimilated into plant biomass and is therefore an important component of the N budget. Modeled N mineralization is a source of uncertainty in simulation outcomes. However, because N mineralization is a large component of available N it is useful to estimate this N source. In computing an N_2O flux rate from Eq. 2, overestimation of N mineralization results in reduced N_2O flux rate estimates while underestimation of N mineralization results in overestimation of N_2O flux rate relative to actual field values. Since we apply the same N mineralization assumptions in our calculation of N_2O flux mass (Eq. 1), the cumulative impact of mis-estimation of N mineralization is minimal.

$$\begin{aligned}&N_2O \text{ flux mass } \left(\text{kg N ha}^{-1}\right) = \\ &N_2O \text{ flux rate } \times \text{ N available } \left(\text{kg N ha}^{-1}\right) \times \text{ duration of management (proportion of season)} \end{aligned} \quad (1)$$

$$N_2O \text{ flux rate } (\textit{p}\text{roportion of N available}) = \frac{\text{observed} N_2O\left(\text{kgNha}^{-1}\text{season}^{-1}\right)}{\text{N available } \left(\text{kg N ha}^{-1} \text{ season}^{-1}\right)}$$

for

$$\begin{aligned}&\text{N Available } = \text{ fertilization } + \text{ gross N mineralization} \\ &\text{season length standardized to 150 days (mean field experiment duration)}\end{aligned} \quad (2)$$

The first input of our accounting model, the N_2O flux rate, is defined in Eq. 2 and is calculated using the published field observations.

Fertilization values were reported in the literature, while gross N mineralization was estimated for each land use based on the 10 year average from simulations using the DNDC model (Tonitto et al. 2007a, b). We used gross N mineralization because these values are recorded as daily outcomes by the DNDC model. Given this accounting framework, the microbes driving the rate of N_2O flux are competing for N with plant uptake, microbial biomass assimilation, nitrate leaching, other N gas flux, and soil N storage. We included N mineralization in our estimate of available N because many of the cropping systems tested do not receive fertilizer and estimating N mineralization allows us to simulate changes in N availability via changes in modeled N mineralization. Outcomes from our N_2O flux mass simulations are of the same magnitude as sampling straight from observed N_2O flux mass values. The advantage of including N mineralization in the N available calculation is that this allows us to test the impact of varying N mineralization rates which is particularly useful for land cover which is not fertilized.

In calculating the N_2O flux rate (Eq. 2) from the observations, the mean N mineralization for each land use type was used; for the simulation of N_2O flux mass (Eq. 1) the N fertilization and N mineralization rates were allowed to vary (described further below). Figure 2 presents the N_2O flux reported in the literature (standardized to units kg N ha^{-1} day^{-1}) compared to the N_2O flux rate (Eq. 2, in units proportion of N available). The data are organized by crop type and climate zone. Data for winter cover crops are predominantly from warmer climate zones,

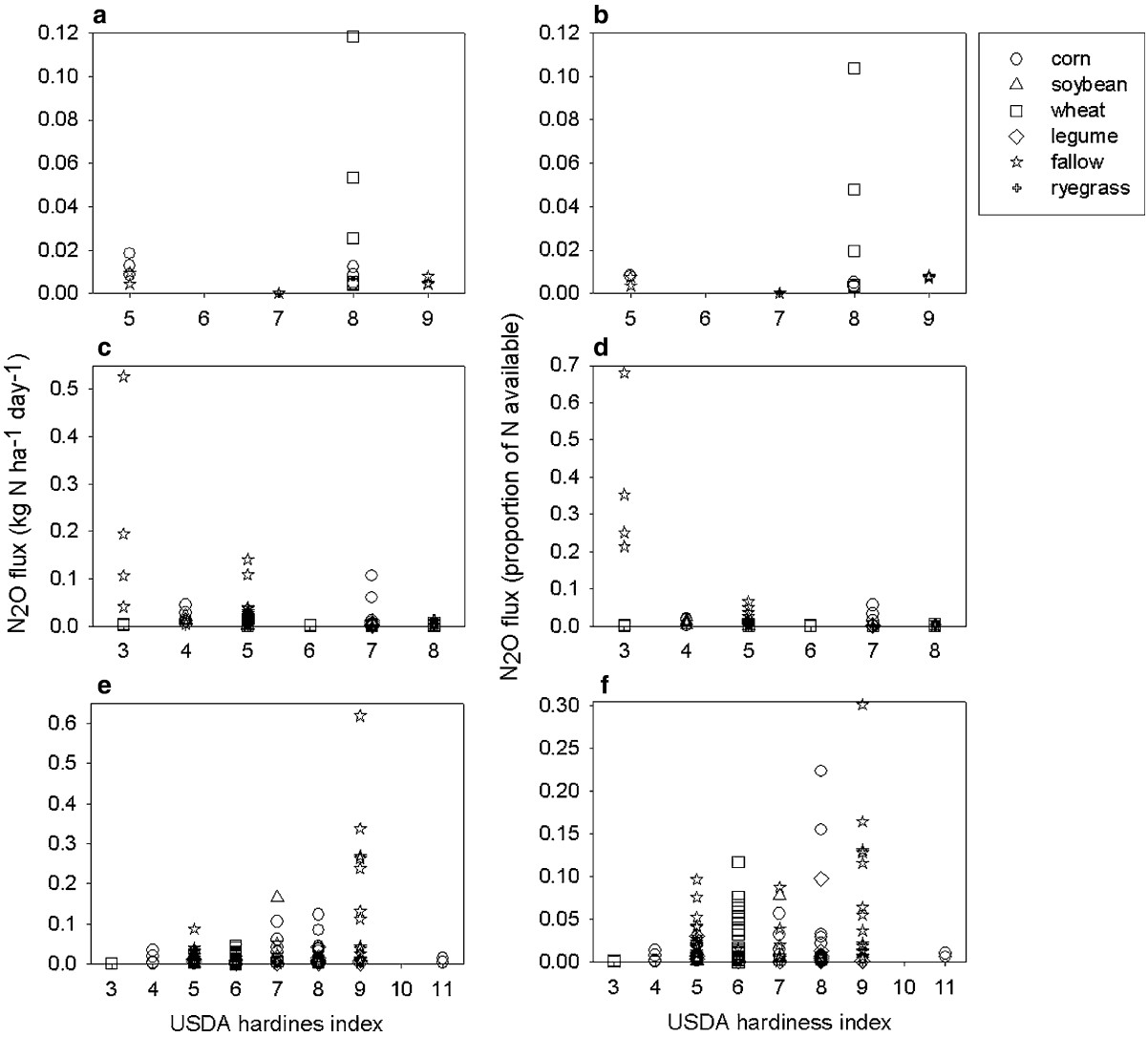

Fig. 2 N_2O flux sorted by crop, soil texture, and USDA hardiness index. Data are presented for fine (**a**, **b**), medium (**c**, **d**), and coarse (**e**, **f**) textured soils. N_2O flux presented in units kg N ha^{-1} day^{-1} (**a**, **c**, **e**) are the values reported in the literature. Seasonal N_2O flux as a proportion of N available (**b**, **d**, **f**) is the flux relationship developed for modeling management of IL rotations. Note that N available varies by land cover type

which is not surprising since land management for winter cover is not promoted by US agricultural policies. The data show the broadest variation under fallow land management, especially in USDA hardiness zone 3.

We simulated the N_2O flux mass (Eq. 1) by computing the N_2O flux rate (Eq. 2) using three different statistical distributions: (1) the lognormal distribution derived using the mean and standard deviation from the literature, (2) the gamma distribution with α and β defined using observed mean and variance (gamma I), and (3) the gamma distribution defined with a lower limit of zero and using observed 50th and 90th percentiles for N_2O flux rate (gamma II). The three statistical distribution assumptions tested are appropriate for describing populations which are positively skewed, with the majority of values close to system mean values, but allowing for high upper tails which reflect observed system variation. The kurtosis values from the observations indicate the data are highly positively skewed. The lognormal distribution provided the best fit to the

observations using both the Anderson–Darling goodness-of-fit metric ($A^2_{corn} = 0.46$, $A^2_{wheat} = 0.1$, $A^2_{ryegrass} = 0.30$ for medium textured soils and $A^2_{legume} = 0.3$, $A^2_{fallow} = 0.66$ for coarse textured soils below the critical test statistics $A^2_{\alpha\ 0.05} = 0.752$) as well as the Kolmogorov–Smirnov metric ($D_{corn} = 0.17$, $D_{wheat} = 0.08$, $D_{ryegrass} = 0.13$ for medium textured soils and $D_{legume} = 0.12$ for coarse textured soils below the critical test statistics $D_{N=30,\ \alpha\ 0.05} = 0.24$). However, other positively skewed distributions, including the gamma and Weibull distributions, were also a good fit. In our model application we included outcomes from the gamma distribution, in addition to the lognormal distribution, because the gamma distribution provides outcomes with shorter upper tail values relative to the lognormal outcomes. Because the database of observations represents limited sampling of the upper tail of the distribution, the lognormal and gamma distributions were applied to provide alternative descriptions of the N_2O flux rate. Figure 3 depicts trends in simulated N_2O flux rate across the three distribution assumptions under corn, soybean, and bare fallow land cover. Mechanistically, the high values in the N_2O flux rate distribution can represent seasons when system climate, crop growth, or land management resulted in a soil environment which favored optimal N_2O flux rates.

We simulated the N available term in Eq. 1 using land-cover-specific rates as follows: (1) For soybean fields we considered available N to be N mineralized and used a value of 130 kg N ha^{-1} per growing season based on the 10 year average from simulations using the DNDC model (Tonitto et al. 2007a, b), (2) For corn and wheat fields, we described mean available N as mineralized N plus recommended N fertilizer applied at a rate of 180 kg N ha^{-1} and 100 kg N ha^{-1}, respectively. Simulated N mineralization averaged 150 kg N ha^{-1} during the corn and wheat growing season, (3) For the ryegrass cover crop and bare fallow we used N available equivalent to a modeled average N mineralization of 100 kg N ha^{-1} based on DNDC simulations, and (4) For the legume system we used an N mineralization rate of 200 kg N ha^{-1} available during legume growth based on DNDC simulations and assumed an N available averaging 150 kg N ha^{-1} following tillage of the legume biomass prior to corn planting (Tonitto et al. 2006). Subsequently, we modeled available N using a normal distribution with mean as indicated above, and standard deviation of 10% of the mean value (Fig. 4). The duration of management term in Eq. 1 followed the time frame reported in Table 1.

Model implementation

We applied a Monte Carlo algorithm using 1,000 iterations to sample from the N_2O flux rate and N available distributions characterized above. These simulated values were then used in Eq. 1 to calculate the potential range of N_2O flux mass (kg N ha^{-1}) across the cropping systems tested. This application assumes that the N_2O flux rate and N available distributions are independent. This assumption is consistent with the observations, which do not support significant linear correlation between field measurements of N_2O flux rate and N available (Fig. 5). For medium textured soils all land cover types (except legume cover) had an $r^2 \leq 0.12$, while legume land cover showed a moderate correlation with an $r^2 = 0.45$. The fine and coarse soil texture regression outcomes showed slight to moderate correlation ($0.15 < r^2 < 0.65$), with wheat land cover demonstrating the most significant correlation. As previously discussed, while laboratory outcomes demonstrate soil environmental controls on N_2O flux rate, the documentation of environmental drivers in the published literature are insufficient to develop a mechanistic model of N_2O flux driven by field conditions. We calculate N available by summing the outcomes from the N fertilization and N mineralization distributions. This assumes that these distributions are independent. This assumption seems biologically reasonable during the fall, winter, and spring. Surrounding the time of fertilization this assumption may be invalid. However, we do not have data to meaningfully model a correlation between N fertilization and N mineralization and believe assuming independence of these distributions is an adequate model.

In our simulations, we used crop type and soil texture as explanatory variables by applying our accounting model using crop and soil texture specific N_2O flux rates and N available. To estimate N_2O flux mass (Eq. 1) over a rotation, flux rates were weighted based on the number of months of a given land management. The N_2O flux for the 6-year-period is then calculated by summing the N_2O flux across each

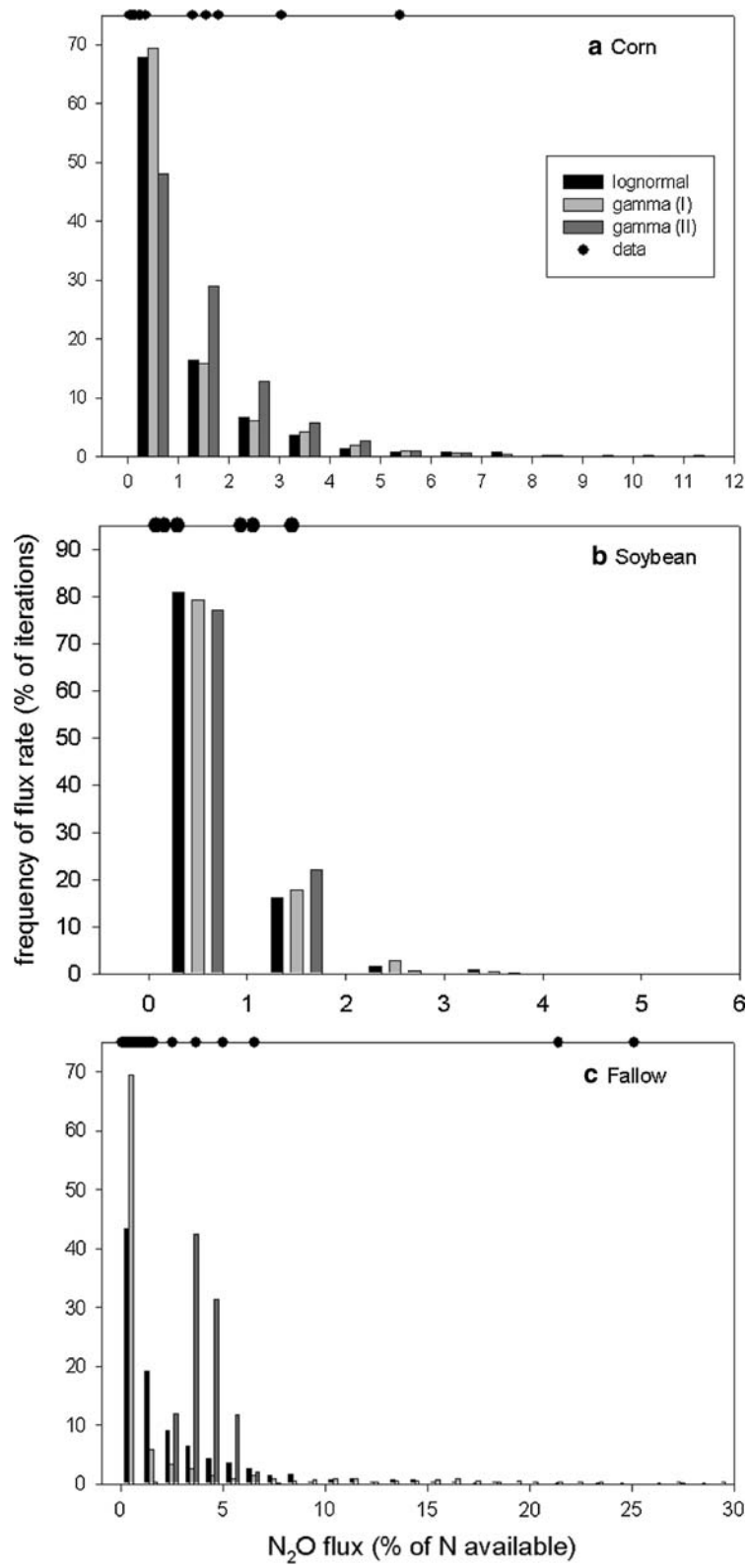

Fig. 3 Seasonal N_2O flux rate for medium textured soil. The histograms show the distribution of simulated N_2O flux rate expressed as a percentage of N available (fertilizer N + mineralized N). Three model distribution assumptions are shown: (1) the lognormal distribution derived from observed mean and standard deviation, (2) the gamma distribution (I) with α and β derived from observed mean and variance, (3) the gamma distribution (II) derived from the 50th and 90th percentiles of the observations. The icons on the upper border of the graph mark individual N_2O flux observations reported in the literature. Graphs present data from **a** corn, **b** soybean, and **c** bare fallow seasons

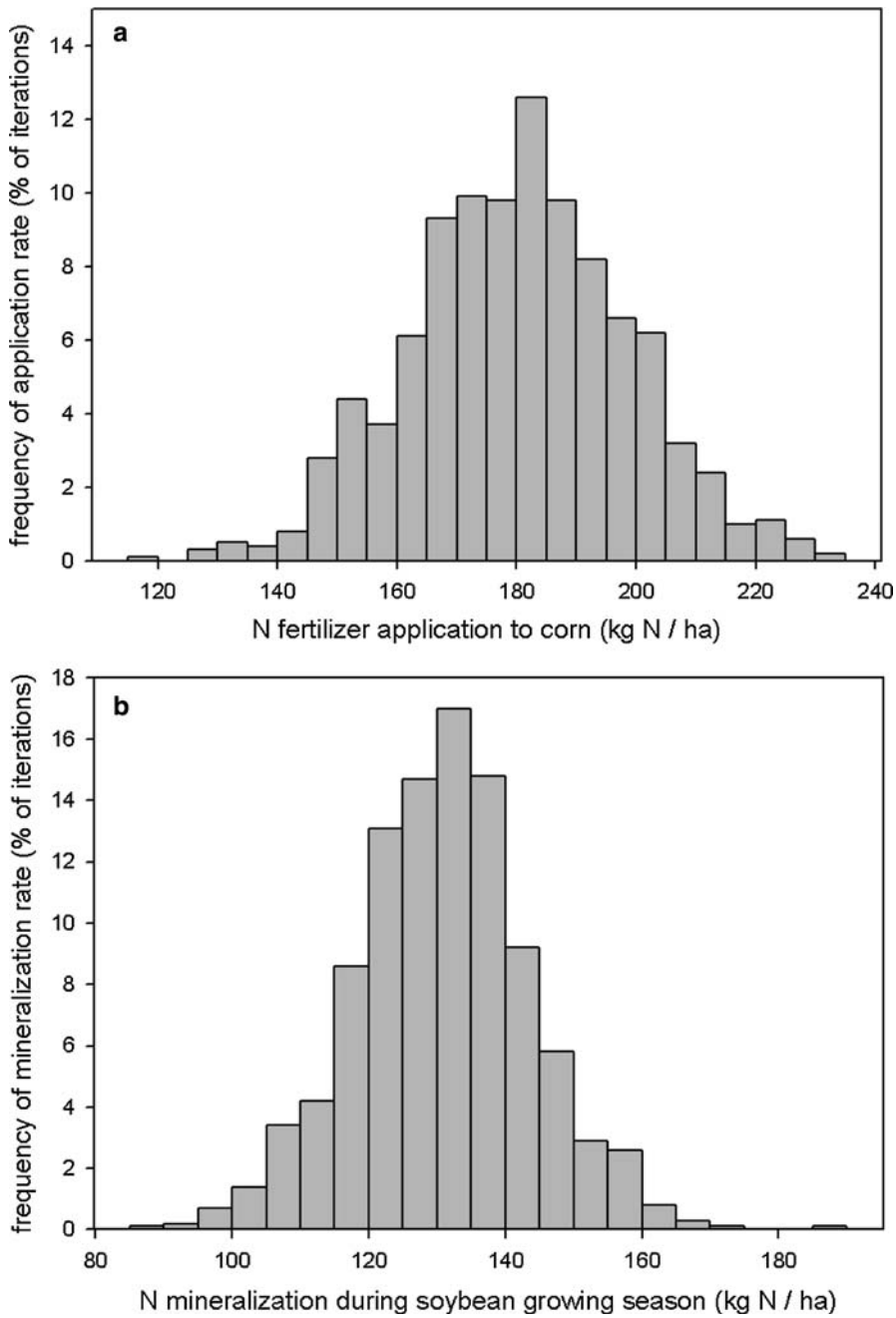

Fig. 4 Simulated distribution of N fertilization and N mineralization. The frequency (% of iterations) of each N level is derived from 1,000 total simulations. **a** Fertilization of corn fields is based on a mean recommended fertilizer level of 180 kg N ha^{-1}. **b** N mineralization under soybean is based on mean outcomes of a 10 year DNDC simulation

land management unit. The cumulative 6 year values are calculated from outcomes of a single Monte Carlo sampling of each relevant land cover type. We chose this approach because we do not know the mechanism which drives the variation in N_2O flux observations. Calculating the 6-year-rotation using multiple Monte Carlo simulations for a given land cover type would imply that the seasonal N_2O flux values are independent, which may be valid if climate was the only driver of variation, but invalid if site properties or land management contribute to N_2O flux variation. While climate is certainly an important determinant of soil environmental conditions, it is not the only driver of N_2O flux.

We present a graphical analysis focused on medium textured soils because this is the only soil

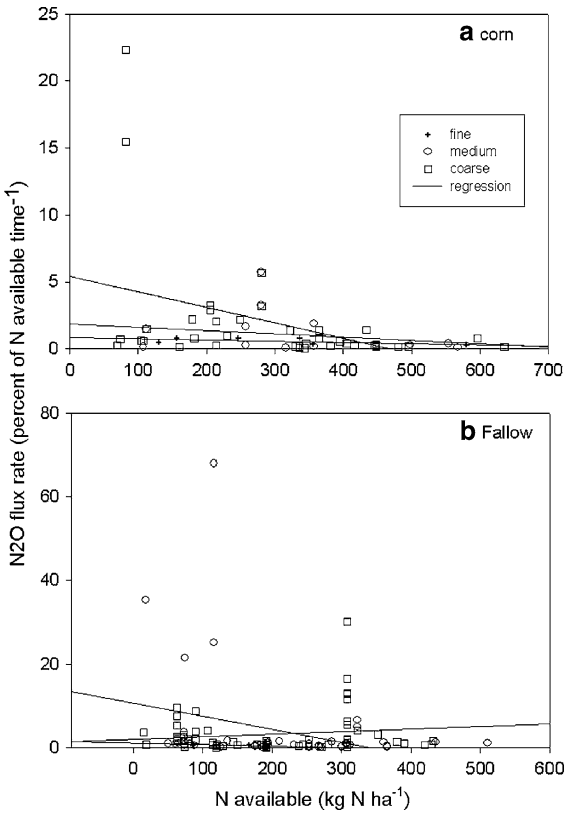

Fig. 5 Linear regression of N available and N_2O flux rate. Observations are presented for corn and fallow land cover, categorized by soil texture

textural class with observations for each land cover type simulated. Additionally, a medium textured soil is the dominant soil texture in the US Corn Belt, and more specifically in Illinois. Our comparison of N_2O flux by rotation for fine and coarse textured soils applied values derived from medium textured soils when the respective textures are missing from the data base. Our model analysis was conducted using CrystalBall 7 software.

Results and discussion

N_2O flux trends

On average, seasonal N_2O flux rate in grain systems as a percent of available N varied from less than 1 to about 4%, while the median seasonal N_2O flux rate was less than 2% (Table 3). The 5 month time frame represents the average length of gas flux sampling in most studies. The absolute highest proportional loss was computed for bare fallow, with corn fields showing the second highest N_2O flux rate (Fig. 3a and c). Flux rates from soybean showed slight variation (Fig. 3b), while little variation in flux rate was observed under ryegrass, wheat, or legume studies conducted on medium textured soils. Overall, coarse textured soils had higher N_2O flux rates than fine textured soils within a given cropping system and demonstrated the highest variation in flux rates. Because we estimated N mineralization using model outcomes, our values for N_2O flux as a percent of N available may differ slightly from the true properties of the agroecosystems studied. However, since we used the same model to derive all of our N

Table 3 Summary statistics of N_2O flux sorted by land cover type and soil texture (fine, medium, coarse). Mean and median N_2O flux as a percent of available N (applied fertilizer N + modeled mineralized N) was quantified for a 5 month period. Number of observations in each category is indicated. (*ND* no data)

Texture	Percent of N available lost as N_2O					
	Corn	Soybean	Wheat	Ryegrass	Legume	Fallow
Fine						
Median	0.5	ND	1.2	ND	ND	0.7
Mean	0.6	ND	3	ND	ND	0.6
Observations	7	ND	6	ND	ND	6
Medium						
Median	0.3	0.6	0.1	0.1	0.2	0.8
Mean	1	0.7	0.2	0.2	0.2	3.9
Observations	15	6	15	29	9	50
Coarse						
Median	0.4	0.2	1.2	ND	0.3	1.3
Mean	1.6	1.3	2.3	ND	1	3.2
Observations	44	8	29	ND	20	59

mineralization values, we expect our estimates of N mineralization to have the same pattern of bias across all simulated land cover categories.

Monte Carlo simulation

Modeled N_2O flux outcomes across the three statistical distributions tested resulted in overlapping patterns of flux, but with important differences with respect to maximum and minimum flux rates (Figs. 3 and 6). Monte Carlo sampling which applied a lognormal distribution or the gamma distribution derived using observed mean and standard deviation (gamma I) accounted for the highest range of predicted N_2O flux (Figs. 3 and 6). In contrast, sampling from a gamma distribution derived from the 50th and 90th percentiles of the observations (gamma II) resulted in outcomes with a smaller range of variation closer to average values. The lognormal and gamma I distributions have many outcomes in the lowest flux ranges, whereas the gamma II distribution has outcomes clustered at intermediate flux values (Figs. 3 and 6). At the high end of flux observations, all statistical models project the 75th percentile of N_2O flux during the corn growing season on medium textured soil to be $\leq$2% of N available (Fig 3a). However, with low probability (<1%) the lognormal model predicted losses up to 35% of available N during the corn growing season. As a result of these low-probability high rates, extreme cumulative N_2O flux exceeding 200 kg N ha^{-1} (per 6 year simulation or 12% of N available) are predicted with very low probability ($\sim$2% of simulations) in the conventional rotation (Fig. 6a). More extreme cumulative N_2O flux ranging from 25 to 30% of N available is predicted in approximately 1% of simulations. However, during the 6 year simulation period, the 75th percentile for the cumulative N_2O flux from a conventional corn-soybean rotation on medium textured soil was $\leq$ 60 kg N ha^{-1} (i.e. 10 kg N ha^{-1} $year^{-1}$) across all statistical distributions tested (Fig. 6a; Table 4). Low variation in legume, wheat, and rye N_2O flux rates under medium textured soil resulted in a narrow range of modeled N_2O flux over the 6 year simulation in the legume rotation on medium textured soil (Fig. 6c).

Fine textured soils showed narrow variation under corn and bare fallow (Fig. 7a, c), but significant variation under wheat (Fig. 7b). Medium textured soils showed little variation under legume, ryegrass, or wheat land cover (with all seasonal N_2O flux rate values <3 kg N ha^{-1}, Table 2), but significant variation under corn (Fig. 7a). Coarse textured soils accounted for the highest flux rates observed and demonstrated high variation across observations (Fig. 7). A comparison across rotations for a medium textured soil using the gamma (II) distribution revealed most cumulative values were <60 kg N ha^{-1} for the 6 year simulation, with cumulative 75th percentile values of 59, 42, and 12 kg N ha^{-1} for conventional, cover crop, and legume rotations, respectively (Fig. 8). The model predicts the highest N_2O flux from the conventional system, with the cover crop rotation demonstrating the next highest cumulative flux values. In contrast, the legume rotation was dominated by 6 year cumulative N_2O flux of less than 20 kg N ha^{-1}. Across all soil textures and statistical distributions modeled, the 25th percentile of average annualized flux rates ranged from 1.7 to 6.7 kg N ha^{-1} in the conventional system, from 1.2 to 4.8 kg N ha^{-1} in the cover crop rotation, and from 0.8 to 5 kg N ha^{-1} in the legume rotation, while the 75th percentile of average annualized flux rates ranged from 2.7 to 12.2 kg N ha^{-1} in the conventional system, from 2.3 to 8.8 kg N ha^{-1} in the cover crop rotation, and from 1.7 to 9.3 kg N ha^{-1} in the legume rotation across all statistical distributions and soil textures studied (Table 4). For a given soil texture, a Kruskal–Wallis test demonstrates that the mean ranks across the three rotations differ significantly for $\alpha = 0.05$ with a $P < 0.0001$. Because soil texture has a significant effect on N_2O flux outcomes, comparing the greenhouse gas implications of a given land management scenario requires detailed knowledge of soil texture and available N.

We simulated N_2O emissions across the three rotations studied using a single Monte Carlo sampling event for each relevant land cover. As discussed in the Methods section, we choose this sampling framework because we do not know the source of variation across field observations. If we assume that all of the variation in field observations is derived from climate, computing N_2O emissions using multiple Monte Carlo sampling events for a given land cover is warranted. We tested model sensitivity to a single versus multiple Monte Carlo sampling event protocol. For each land cover type, we compared predicted N_2O emissions resulting from two seasons

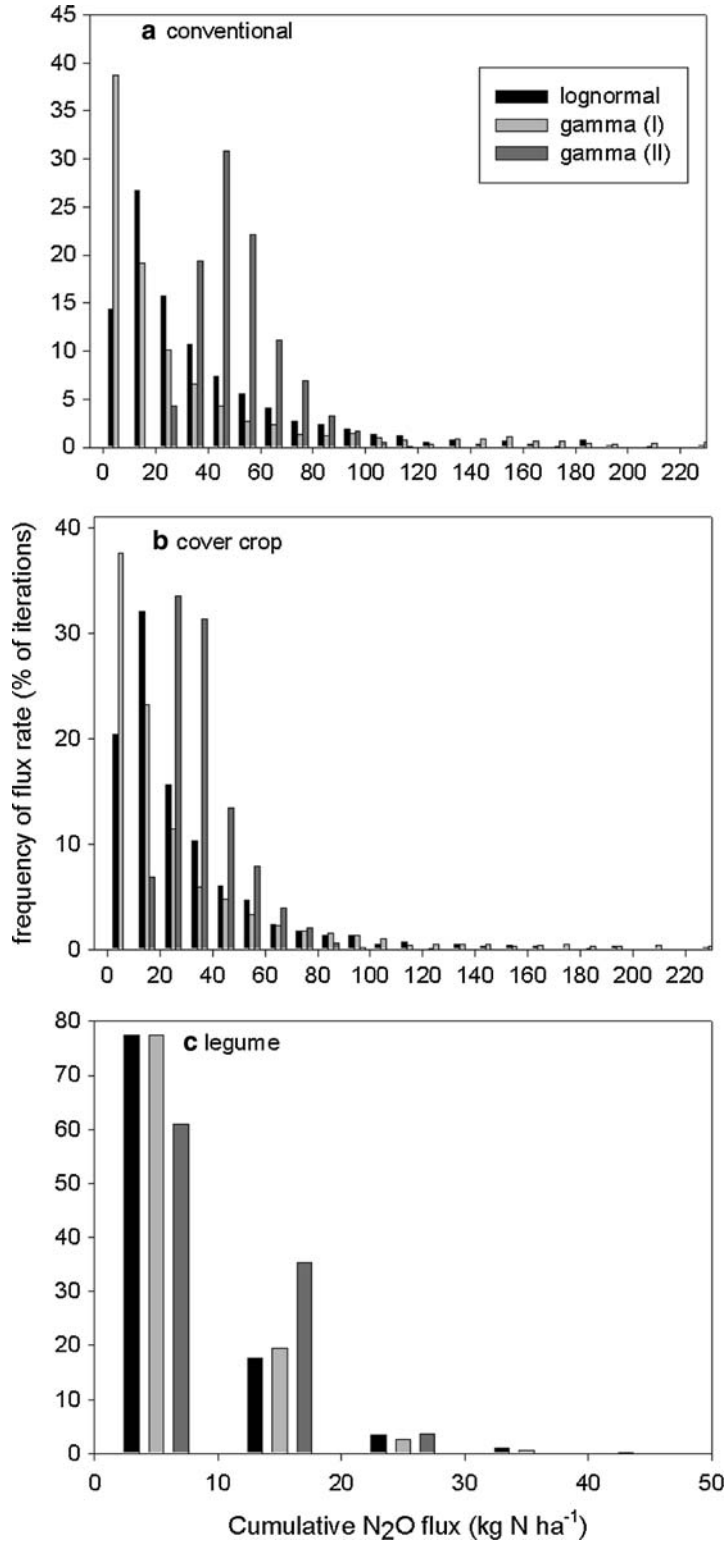

Fig. 6 Cumulative 6 year N_2O flux (kg N ha^{-1}). Simulation results from three probability distributions (lognormal, gamma (I), gamma (II)) are compared for **a** conventional, **b** cover crop, and **c** legume rotations on medium textured soil

Table 4 Average annualized N_2O flux (kg N ha^{-1} $year^{-1}$) resulting from a 6 year simulation

	Rotation								
	Conventional			Cover crop			Legume		
	25th percentile	50th percentile	75th percentile	25th percentile	50th percentile	75th percentile	25th percentile	50th percentile	75th percentile
Lognormal									
Fine	1.7	2.2	2.7	1.5	1.8	2.3	2.2	3.3	5.7
Medium	2.2	4.2	8.3	1.8	3.2	5.8	0.8	1.2	1.7
Coarse	3.0	5.3	9.8	2.3	4.0	7.2	2.8	4.5	6.8
Gamma (I)									
Fine	1.7	2.2	2.7	1.5	2.0	2.3	1.3	2.8	6.7
Medium	1.0	2.5	6.8	1.2	2.3	5.7	0.8	1.2	1.7
Coarse	1.5	4.3	10.2	1.3	3.2	7.2	2.0	4.2	7.8
Gamma (II)									
Fine	2.0	2.3	2.7	1.8	2.2	2.3	3.2	5.2	8.0
Medium	6.7	8.0	9.8	4.3	5.5	7.0	1.2	1.5	2.0
Coarse	6.2	8.7	12.2	4.8	6.7	8.8	5.0	7.2	9.3

Outcomes are summarized using the 25th, 50th, and 75th percentile values for each rotation (conventional, cover crop, legume), for each statistical distribution tested (lognormal, gamma (I), gamma (II)), across all soil textural classes (fine, medium, coarse)

of a land cover computed using one Monte Carlo sampling event versus two sampling events. The 25th through 75th percentile outcomes are equivalent under either sampling scenario (Table 5). The main effect of multiple Monte Carlo sampling events is to reduce the probability of extremely low or extremely high cumulative flux values. Essentially, it becomes improbable for there to be two draws of the lowest or highest N_2O flux distribution.

Forecasting N_2O flux

Modeling N_2O flux remains a significant challenge. Discrepancies exist in regional upscaling of N gas flux predictions across empirical and process model approaches. Empirical modeling draws heavily from mean dynamics, largely ignoring peak events (Hofstra and Bouwman 2005; Stehfest and Bouwman 2006), leading to annual predictions of between 2 and 4 kg N ha^{-1} losses from the US Corn Belt. Process models applied to Illinois predict similarly low N_2O flux rates in some years (David et al. 2009). Likewise, the application of DAYCENT at the US national scale (del Grosso et al. 2006) resulted in an annual average N_2O flux prediction of <3 kg N ha^{-1} for the state of Illinois. However, even when annual flux rates are similar across process models, the seasonal dynamics can be very different, indicating model dynamics are predicting N gas flux as a result of different mechanisms (David et al. 2009).

While process model annual outcomes overlap with empirical model projections in some simulation years, process models can also predict extremely high N_2O flux rates ranging from 10 to 40 kg N ha^{-1} in high flux years (Tonitto et al. 2007b). Most of the N_2O and N_2 flux predicted in process models occurs during extreme pulse events, with highest N_2O flux projections occurring in years with low simulated nitrate leaching. Our toolbox for aggregating peak N_2O flux events remains limited, especially since accurately modeling the partitioning of N_2:N_2O is highly dependent on modeling soil moisture status. Additionally, many agroecosystem models do not partition between N_2 and N_2O flux (e.g., DRAINMOD-N, EPIC, SWAT), which means we must include alternative tools to ask questions about agricultural policy and greenhouse gas emissions. Further field observation is necessary to quantify the extent to which pulsed events contribute to N_2O flux at the landscape scale.

The low probability, high N_2O flux predicted in this analysis is similar to the extreme N_2O flux outcomes ranging from 12 to 49 kg N ha^{-1} $year^{-1}$ simulated in DNDC model application to corn-

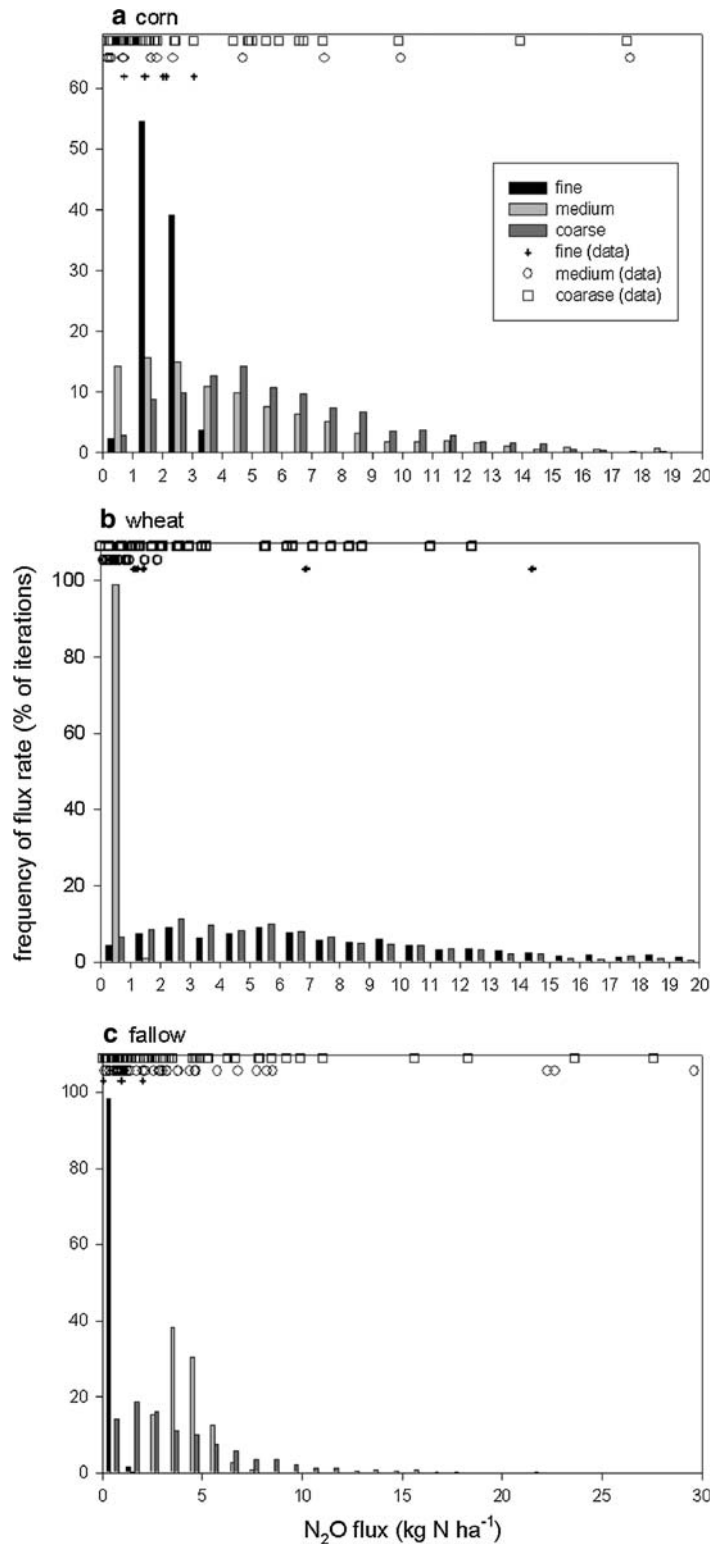

Fig. 7 Growing season N_2O flux (kg N ha^{-1}). The histograms show simulated N_2O flux during **a** the corn growing season, **b** the wheat growing season, and **c** bare fallow for each soil textural class using the gamma distribution (II). The icons on the upper portion of the graph mark individual N_2O flux observations (sorted by soil texture)

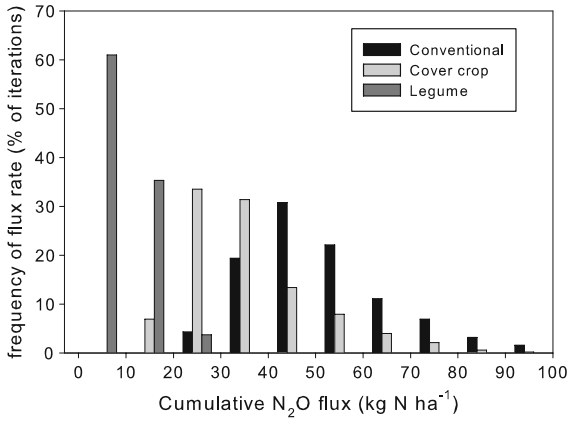

Fig. 8 N_2O flux across rotations. Simulated 6 year cumulative N_2O flux (kg N ha^{-1}) using the gamma distribution (II) is shown for each cropping system under medium textured soil

soybean rotations with winter bare fallow (David et al. 2009). Field experiments which target event sampling, such as N gas flux when fertilization coincides with heavy precipitation, likewise indicates extreme peak N gas flux is possible (Dobbie and Smith 2001; Li et al. 2002; Wagner-Riddle and Thurtell 1998). However, we do not have observations to verify or disprove the possibility of extremely high flux years in the Illinois agricultural landscape. Outcomes from the Monte Carlo sampling presented here as well as mechanistic simulation models both predict the possibility of very high N_2O loss. However, high N_2O flux events should be infrequent; multi-year high N_2O flux predictions simulated by the DNDC model (David et al. 2009) highlights our limited ability to predict N_2O flux.

Conclusions

The Monte Carlo sampling approach presented here is an empirical approach that accounts for the full range of N_2O flux rates observed under field conditions from relevant published studies. Because studies are conducted under a broad range of conditions, this modeling approach is an empirical tool for approximating the response of N_2O flux rates to diverse environmental conditions. As the available temporal and spatial coverage of N_2O flux data increases, we can repeat our simulations and ask whether the new data changes the shape of the predicted distributions. Continued support for N gas flux data collection is necessary to increase our understanding of ecosystem dynamics as well as to validate or refute model outcomes.

Acknowledgments This paper is a product of a workshop on Denitrification Modeling Across Terrestrial, Freshwater, and Marine Systems; held November 28–30, 2006, at the Institute of Ecosystem Studies, Millbrook, NY, with support from the Denitrification Research Coordination Network of the National Science Foundation, award DEB0443439 and the Northeastern States Research Cooperative (Grant # 02-CA-11242343-105). We thank the co-chairs Sybil Seitzinger, Eric Davidson, Peter Groffman, Elizabeth Boyer, and Rosalynn Lee for organizing the workshop. Support for this research was provided by an NSF Biocomplexity in the Environment/Coupled Natural-Human Cycles Program (Grant # 0508028 to Drinkwater

Table 5 Cumulative N_2O flux predicted for two seasons of a given land cover category using one versus two Monte Carlo sampling events. Simulations are conducted by land cover type for medium textured soil using the gamma (II) distribution

Monte Carlo events	N_2O flux (kg N ha^{-1}) by land cover					
	Corn	Soybean	Fallow	Ryegrass	Wheat	Legume
1-draw						
Minimum	0.04	0.10	2.61	0.01	0.08	0.07
25th percentile	3.40	1.12	6.40	0.25	0.56	0.42
50th percentile	6.89	1.73	7.66	0.48	0.78	0.58
75th percentile	12.75	2.48	9.09	0.82	1.04	0.79
Maximum	53.78	8.17	14.91	3.19	2.93	1.84
2-draws						
Minimum	0.38	0.40	3.60	0.02	0.26	0.13
25th percentile	5.04	1.39	6.81	0.29	0.64	0.35
50th percentile	8.29	1.82	7.83	0.46	0.79	0.45
75th percentile	12.19	2.37	8.90	0.72	0.97	0.56
Maximum	37.54	5.02	12.95	2.51	1.83	1.14

et al.) and a modeling grant from the Cornell University Agricultural Ecosystems Program: Understanding Sources and Sinks of Nutrients and Sediment in the Upper Susquehanna River Basin funded by the USDA CSREES program (award # 2005-34244-15740). The authors are grateful to Peter Woodbury and anonymous reviewers for insightful comments on an earlier draft of the manuscript.

References

Arnold JG, Srinivasan R, Muttiah RS, Williams JR (1998) Large area hydrologic modeling and assessment part I: model development. J Am Water Resour Assoc 34:73–89

Cavigelli MA, Robertson GP (2000) The functional significance of denitrifier community composition in a terrestrial ecosystem. Ecol 81(5):1402–1414

Clemens J, Schillinger MP, Goldbach H, Huwe B (1999) Spatial variability of N_2O emissions and soil parameters of an arable silt loam—a field study. Biol Fertility Soils 28:403–406

David MB, Gentry LE (2000) Anthropogenic inputs of nitrogen and phosphorus and riverine export for illinois, USA. J Environ Qual 29:494–508

David MB, Del Grosso SJ, Hu X, McIsaac GF, Parton WJ, Marshall EP, Tonitto C, Youssef MA (2009) Modeling denitrification in a tile-drained, corn and soybean agroecosystem of Illinois, USA. Biogeochem. doi:10.1007/s10533-008-9273-9

Del Grosso SJ, Parton WJ, Mosier AR, Walsh MK, Ojima DS, Thornton PE (2006) DAYCENT national-scale simulations of nitrous oxide emissions from cropped soils in the united states. J Environ Qual 35:1451–1460

del Prado A, Merino P, Estavillo JM, Pinto M, Gonzalez-Murua C (2006) N_2O and NO emissions from different N sources and under a range of soil water contents. Nutr Cycling Agroecosyst 74:229–243

Dobbie KE, Smith KA (2001) The effects of temperature, water-filled pore space and land use on N_2O emissions from an imperfectly drained gleysol. Eur J Soil Sci 52:667–673

Drinkwater LE , Snapp SS (2007) Nutrients in agroecosystems: rethinking the management paradigm. Adv Agron 92: 163–186

Firestone MK, Davidson EA (1989) Microbiological basis for NO and N_2O production and consumption in soils. In: Andreae MO, Schimel DS (eds) Exchange of trace gases between terrestrial ecosystems and the atmosphere. Wiley, Chichester, pp 7–21

Gassman PW, Williams JR, Benson VW, Izaurralde RC, Hauck L, Jones CA, Atwood JD, Kiniry J, Flowers JD (2005) Historical development and applications of the EPIC and APEX models. Working paper 05-WP 397 Center for Agricultural and Rural Development, Iowa State University, Ames, IA (available on-line http://wwwcardiastate edu/publications/DBS/PDFFiles/05wp397pdf)

Groffman PM, Altabet MA, Bohlke JK, Butterbach-Bahl K, David MB, Firestone MK, Giblin AE, Kana TM, Nielsen LP, Voytek MA (2006) Methods for measuring denitrification: diverse approaches to a difficult problem. Ecol Appl 16:2091–2122

Heinen M (2006) Simplified denitrification models: overview and properties. Geoderma 133:444–463

Hofstra N, Bouwman AF (2005) Denitrification in agricultural soils: summarizing published data and estimating global annual rates. Nutr Cycling Agroecosyst 72:267–278

Li CS, Frolking S, Frolking TA (1992) A model of nitrous-oxide evolution from soil driven by rainfall events.1. model structure and sensitivity. J Geophys Res Atmos 97:9759–9776

Li X, Inubushi K, Sakamoto K (2002) Nitrous oxide concentrations in an andisol profile and emissions to the atmosphere as influenced by the application of nitrogen fertilizers and manure. Biol Fertility Soils 35:108–113

Li Y, Chen DL, Zhang YM, Edis R, Ding H (2005) Comparison of three modeling approaches for simulating denitrification and nitrous oxide emissions from loam-textured arable soils. Global Biogeochem Cycles 19:GB3002

Li Y, White R, Chen DL, Zhang JB, Li BG, Zhang YM, Huang YF, Edis R (2007) A spatially referenced water and nitrogen management model (WNMM) for (irrigated) intensive cropping systems in the north china plain. Ecol Model 203:395–423

Mathieu O, Leveque J, Henault C, Milloux MJ, Bizouard F, Andreux F (2006) Emissions and spatial variability of N_2O, N-2 and nitrous oxide mole fraction at the field scale, revealed with N-15 isotopic techniques. Soil Biol Biochem 38:941–951

McSwiney CP, Robertson GP (2005) Nonlinear response of N_2O flux to incremental fertilizer addition in a continuous maize (zea mays L.) cropping system. Global Change Biol 11:1712–1719

Mosier AR, Duxbury JM, Freney JR, Heinemeyer O, Minami K (1996) Nitrous oxide emissions from agricultural fields: assessment, measurement and mitigation. Plant Soil 181: 95–108

Neitsch SL, Arnold JG, Kiniry JR, Williams JR, King KW (2005) Soil and water assessment tool user's manual. TWRI Report TR-191, Texas Water Resour Inst College Station, Texas

Parton WJ, Schimel DS, Cole CV, Ojima DS (1987) Analysis of factors controlling soil organic-matter levels in great-plains grasslands. Soil Sci Soc Am J 51:1173–1179

Parton WJ, Hartman M, Ojima D, Schimel D (1998) DAYCENT and its land submodel: description and testing. Global Planetary Change 19:35–48

Rykiel EJ (1996) Testing ecological models: the meaning of validation. Ecol Model 90:229–244

Stehfest E, Bouwman L (2006) N_2O and NO emission from agricultural fields and soils under natural vegetation: summarizing available measurement data and modeling of global annual emissions. Nutr Cycling Agroecosyst 74: 207–228

Tague CL, Band LE (2004) RHESSys: regional hydro-ecologic simulation system- an object-oriented approach to spatially distributed modeling of carbon, water, and nutrient cycling. Earth Interact 8:1–42

Tonitto C, David MB, Drinkwater LE (2006) Replacing bare fallows with cover crops in fertilizer-intensive cropping

systems: a meta-analysis of crop yield and N dynamics. Agric Ecosyst Environ 112:58–72

Tonitto C, David MB, Drinkwater LE, Li CS (2007a) Application of the DNDC model to tile-drained illinois agroecosystems: model calibration, validation, and uncertainty analysis. Nutr Cycling Agroecosyst 78:51–63

Tonitto C, David MB, Li CS, Drinkwater LE (2007b) Application of the DNDC model to tile-drained illinois agroecosystems: model comparison of conventional and diversified rotations. Nutr Cycling Agroecosyst 78:65–81

Wagner-Riddle C, Thurtell GW (1998) Nitrous oxide emissions from agricultural fields during winter and spring thaw as affected by management practices. Nutr Cycling Agroecosyst 52:151–163

Wallenstein MD, Myrold DD, Firestone M, Voytek M (2006) Environmental controls on denitrifying communities and denitrification rates: insights from molecular methods. Ecol Appl 16:2143–2152

Weier KL, Doran JW, Power JF, Walters DT (1993) Denitrification and the dinitrogen nitrous-oxide ratio as affected by soil-water, available carbon, and nitrate. Soil Sci Soc Am J 57:66–72

Williams JR, Dyke PT, Jones CA (1983) EPIC: a model for assessing the effects of erosion on soil productivity. In: Laurenroth WK et al (eds) Analysis of ecological systems: state-of-the-art in ecological modeling. Elsevier Scientific Publishing Company, Amsterdam, pp 553–572

Youssef MA (2003) Modeling nitrogen transport and transformations in high water table soils. Ph.D. disseration. North Carolina State University, Raleigh, NC

Youssef MA, Skaggs RW, Chescheir GM, Gilliam JW (2005) The nitrogen simulation model, DRAINMOD-N II. Trans ASAE 48:611–626